Ecotoxicology and Environmental Safety 303 (2025) 119016



Contents lists available at ScienceDirect

Ecotoxicology and Environmental Safety

journal homepage: www.elsevier.com/locate/ecoenv





Multi-frequency electromagnetic radiation promoted hepatic lipid metabolism via the adiponectin pathway in mice

Jing Xu [a,b], Xinyu Wang [a], Menghua Li [a], Lihui Zhang [a], Xuelong Zhao [a], Guofu Dong [a,*], Changzhen Wang [a,*]

[a] Beijing Key Laboratory for Radiobiology, Beijing Institute of Radiation Medicine, Beijing 100850, China
[b] School of Life Sciences, Hebei University, Baoding 071000, China

ARTICLE INFO

Edited by G Liu

Keywords:
Multi-frequency RF-EMR
Lipid metabolism
Adiponectin
HFD

ABSTRACT

Radiofrequency electromagnetic radiation (RF-EMR) is ubiquitous in daily life, and the complexity of the electromagnetic environment continues to increase. Nevertheless, research on the biological effects of compound radiofrequency radiation—particularly its influence on lipid metabolism under realistic exposure scenarios—remains limited, and the underlying mechanisms are not yet fully elucidated. To investigate the impact of compound radiofrequency radiation on lipid metabolism, multi-frequency radiation exposure model both normal and obese mice were established. Our findings indicated that prolonged exposure to composite three-frequency radiation led to a significant reduction in serum levels of TG and LDL, accompanied by an increase in HDL. Concurrently, we observed upregulation of UCP1 expression and enhanced lipid metabolic activity in adipose tissue. Furthermore, radiation exposure promoted the secretion of adiponectin and other adipokines from adipose tissue. These adipokines subsequently activated the adiponectin signaling pathway in the liver, stimulated fatty acid β-oxidation while suppressed lipogenesis. In the obesity model, long-term exposure to compound three-frequency radiation similarly enhanced lipid metabolism in adipose tissue and stimulated adiponectin secretion. This subsequently activated the adiponectin signaling pathway in the liver, led to improved hepatic lipid homeostasis and a reduction in the severity of both hepatic steatosis and fibrosis. Taken together, these findings demonstrated that compound radiofrequency radiation enhanced lipid metabolism in adipose tissue and liver through adiponectin-mediated mechanisms, thereby promoted systemic metabolic regulation.

1. Introduction

Radiofrequency electromagnetic radiation (RF-EMR) is the most prevalent form of electromagnetic exposure in daily life, including high-frequency electromagnetic fields and microwaves, which emitted by communication devices and household appliances across various frequency bands (Mortazavi et al., 2014; Koppel et al., 2022). In recent years, growing concern has emerged among researchers regarding the potential health implications of RF-EMR. Studies have reported associations between RF-EMR exposure and adverse health effects such as dizziness, headache, anxiety, depression, heart palpitations, endocrine disorders and reproductive disorders (Levitt and Lai, 2010; Hardell and Koppel, 2022; Küçer and Pamukçu, 2014; Men et al., 2023; Yu et al., 2020). Many of these physiological alterations are closely linked to metabolic disturbances. Consequently, we thought it is necessary to study the mechanism of radiofrequency electromagnetic radiation affecting lipid metabolism.

Obesity has long been recognized as a major global health concern associated with various physiological complications, including cardiovascular disease (Caballero, 2019). Adipose tissue and the liver play central roles in lipid metabolism, which is related to obesity. Based on cellular composition and function, adipose tissue is classified into two main types: brown adipose tissue (BAT) and white adipose tissue (WAT). Brown adipocytes are characterized by a high density of mitochondria, which facilitate the conversion of energy stored in lipid droplets into heat, thereby contributing to the maintenance of normal body temperature (Liu et al., 2023; Ahmad et al., 2021). However, BAT undergoes progressive degeneration with advancing age. Both the activity and mass of BAT exhibit a negative correlation with obesity levels. Enhancing BAT activity may therefore represent a promising therapeutic strategy for mitigating obesity and reducing the risk of associated metabolic disorders, such as cardiovascular diseases (Chand et al.,

* Corresponding authors.
E-mail addresses: dongguofu052@126.com (G. Dong), wangcz2002@aliyun.com (C. Wang).

https://doi.org/10.1016/j.ecoenv.2025.119016
Received 5 June 2025; Received in revised form 2 September 2025; Accepted 3 September 2025
Available online 6 September 2025
0147-6513/© 2025 The Authors. Published by Elsevier Inc. This is an open access article under the CC BY-NC-ND license (http://creativecommons.org/licenses/by-nc-nd/4.0/).

2024). Current research indicated that cold exposure (Xiao et al., 2023), exercise (Chen et al., 2022), and dietary interventions (Xue et al., 2024) can promote the browning of white adipose tissue (WAT), thereby enhancing oxidative phosphorylation within WAT. Improving hepatic metabolism has also been shown to ameliorate numerous obesity-related pathologies (Karpale et al., 2023). However, there remains a scarcity of in-depth studies investigating the physiological alterations and underlying mechanisms in both liver and adipose tissues following exposure to radiofrequency radiation.

Lipid metabolism encompasses both the catabolism and anabolism of lipids. Triglycerides constitute the most abundant lipid species within adipocytes. During fasting states, triglycerides mobilized from adipose tissue are transported to the liver via lipoproteins. In the liver, they undergo β-oxidation to produce acetyl-CoA, which subsequently enters the tricarboxylic acid (TCA) cycle to generate energy for the body (Magkos, Mittendorfer, 2009). In addition to triglyceride synthesis, lipid anabolism also contributes to the production of hormones and structural lipids for cellular components. Studies have indicated that mobile phone electromagnetic radiation accelerated glucose consumption and promoted catabolic processes in the brain (Volkow et al., 2011). Furthermore, some researchers have reported that radiofrequency radiation may enhanced fatty acid metabolism (Fragopoulou et al., 2018; Furtado-Filho et al., 2014). However, while numerous studies have described alterations in indicators of carbohydrate and lipid metabolism following radiofrequency radiation exposure, the specific effects and underlying mechanisms of such radiation on lipid metabolic pathways remain poorly understood and insufficiently investigated.

Adiponectin, an endogenous bioactive peptide predominantly secreted by adipocytes, exhibits multiple biological functions such as anti-diabetic, anti-atherosclerotic, and anti-inflammatory activities (Vaidya et al., 2013; Miyagishima et al., 2007; Choi et al., 2020). It exerts these effects by binding to specific receptors, leading to the modulation of key enzymes involved in metabolic pathways in terms of their expression levels or catalytic activities (Kadowaki et al., 2006). This process ultimately influences the concentration of metabolic end-products, thereby regulating both lipid and carbohydrate metabolism. The liver, a central organ in systemic metabolism, represents a major target of adiponectin action. Upon transportation through the bloodstream, adiponectin binds to hepatic adiponectin receptors, where it enhances carbohydrate and lipid metabolism while simultaneously suppressing fatty acid synthesis (Ghadge et al., 2018; Dyck et al., 2006).

In this study, we observed that compound radiofrequency electromagnetic radiation exposure reduced the rate of body weight gain in mice. Further analysis suggested the potential involvement of the adiponectin signaling pathway in the regulation of hepatic lipid metabolism. Based on these findings, we extended our investigation to high-fat diet mice subjected to compound radiofrequency radiation. The results demonstrated that radiation exposure also attenuated weight gain in this model and indicated that adiponectin participates in the modulation of lipid metabolism during radiation treatment. In conclusion, our findings indicated that adiponectin pathways are involved in the regulation of lipid metabolism in adipose tissue under compound radiofrequency radiation exposure. This process promoted fatty acid catabolism in the liver and enhanced triglyceride breakdown as well as oxidative phosphorylation capacity in adipose tissue.

2. Materials and methods

2.1. Animals and treatments

Specific pathogen free (SPF) male C57BL/6 mice (5–8 weeks, SPF (Beijing) Biotechnology Co., Ltd.) were housed in a standard environment with five animals per cage and provided ad libitum access to food and water (room temperature: 22–24°C; 12-h light/dark cycle: lights on from 09:00–21:00; relative humidity: 50–60 %). After a 7-day acclimatization period, the mice were assigned to different experimental groups. In the first experiment(n = 20): Control(n = 10), RF-EMR (n = 10). In the second experiment, new mice were divided into four groups(n = 40): Control(n = 10), HFD(n = 10), RF-EMR (n = 10) and RF-HFD (n = 10). The HFD group and RF-HFD group mice were fed high-fat diet that contains 20 % kcal protein, 20 % kcal carbohydrates and 60 % kcal fat (H10060, Beijing HFK Bio-Technology. co., LTD China) from 5 weeks of age for 3 months, Mice in the Control and RF-EMR groups were maintained on a standard diet for the same period prior to radiation exposure.

2.2. RF-EMR Exposure

In the first experiment, the RF-EMR group was exposed to multi-frequency RF-EMR (0.9, 1.5 and 2.65 GHz) that each frequency was irradiated for 40 min for total of 2 h per day with SAR of 4.0 W/kg. The Control group was handled identically but without exposure. After 3 weeks of exposure, mice were euthanized for morphological and biochemical analyses. The experimental irradiation system which is capable of conducting whole-body irradiation experiments on animals within the 0.8–4 GHz frequency band includes an RF Signal Generator (RIGOL Technologies, Inc., China), a radiofrequency power amplifier (Nanjing Nate Communication Electronics Co., Ltd., China), an antenna selector, a control computer, and an irradiation box (Fig.S1B). The shield walls are made of metallic mesh allowing for ventilation and heat dissipation. During exposure, mice were housed individually in ventilated acrylic containers (8.4 × 6.7 × 5.4 cm^3) that permitted free movement. In the second experiment, both the RF-EMR and RF-HFD groups underwent the same irradiation protocol as in the first experiment (2 h/day, SAR = 4.0 W/kg, multi-frequency sequential exposure). The Control and HFD groups were subjected to identical handling conditions without exposure. After 4 weeks, all mice were sacrificed for subsequent morphological and biochemical studies.

2.3. Body weight monitoring and serum lipid biochemistry

During the exposure period, the body weight of the mice in each group was monitored on a weekly basis. Upon completion of the irradiation protocol, all animals were euthanized and serum levels of lipid metabolism indicators—including high-density lipoprotein (HDL), low-density lipoprotein (LDL), total cholesterol (TCHO), and triglycerides (TG)—were quantified using an automated blood biochemistry analyzer.

2.4. Western blotting

The adipose tissue and liver samples were homogenized in ice-cold RIPA lysis buffer (Beijing Biomed Genetic Technologies Limited, Beijing China) containing 50 mM pH 7.4 Tris-HCl, 2 mM EDTA, 1 % Triton X-100, 0.1 % SDS, 1 % sodium deoxycholate, 1 mM sodium orthovanadate, 1 mM sodium fluoride, 150 mM and 1 ×protease inhibitor cocktail (Sigma-Aldrich, St. Louis, MO, USA). Then the homogenates were centrifuged at 12000 g for 15 min in 4 ∘C. Protein concentration in the supernatant was determined using a BCA assay kit (Thermo Fisher Scientific Inc., USA). Proteins were separated by sodium dodecyl sulfate-polyacrylamide gel electrophoresis (SDS-PAGE) via 10 % Separating glue and transferred to PVDF membranes. The membranes were blocked with 5 % skim milk for 2 h at room temperature and then incubated overnight at 4 °C with specific primary antibodies diluted in 5 % skim milk. The following day, membranes were washed and incubated with horseradish peroxidase (HRP)-conjugated secondary antibodies for 1 h at room temperature. Protein bands were visualized using an ECL Plus luminescent substrate (Beijing Lablead Biological Technology Co., Beijing, China) and chemiluminescence imaging system (Sewell Biotechnology Co., Ltd, China). Band intensities were quantified using ImageJ software. Details regarding the primary and secondary antibodies used are provided in Table S1.

2.5. Hematoxylin-Eosin staining (HE)

Fresh adipose tissue and liver tissues were fixed, dehydrated, and embedded in paraffin. Subsequently, the embedded tissues were sectioned at a thickness of 4 μm. Following routine deparaffinization and rehydration, the paraffin sections were stained with hematoxylin and eosin (H&E). The stained sections were examined under a light microscope (OLYMPUS BX41; Olympus Corporation, Japan) at 400 × magnification, and images were captured using the NIS-Elements F 3.0 imaging system (Nikon Corporation, Japan). Quantitative analysis of the histological data was performed using ImageJ software (National Institutes of Health, USA).

2.6. Masson three-color staining

Paraffin sections of adipose tissue and liver were stained using a Masson staining kit (Shanghai Beibo Biotechnology Co., Ltd., China). The staining procedure consisted of the following steps: deparaffinization and hydration of sections, fixation with Bouin's solution, staining with Lapis Lazuli blue, hematoxylin counterstaining, differentiation with acidic ethanol, Ponceau red staining, treatment with phosphomolybdic acid, aniline blue staining, weak acid rinsing, followed by dehydration and mounting. The stained sections were examined under a light microscope (OLYMPUS BX41; Olympus Corporation, Japan) at 400 × magnification, and images were acquired using the NIS-Elements F 3.0 software (Nikon Corporation, Japan). Quantitative analysis of staining results was performed using ImageJ software (National Institutes of Health, USA).

2.7. Enzyme linked immunosorbent assay (ELISA)

According to the manufacturer's instructions, the levels of Acetyl-CoA (ACA) and Malonyl-CoA (MCA), as well as the enzymatic activities of Acetyl-CoA Carboxylase (ACC) and Carnitine Palmitoyl transferase (CPT) in adipose and liver tissues, were quantified using commercially available ELISA kits and enzyme activity assay kits (Shanghai Meilian Biological Technology Co. Ltd., China). Absorbance measurements were performed using a SpectraMax iD3 multifunctional microplate reader (Molecular Devices, USA) for data acquisition.

2.8. Quantitative real-time PCR (qRT-PCR)

Total RNA was extracted from adipose tissue and liver using the TRIzol method. The procedure involved homogenizing the tissue to disrupt cells, followed by RNA isolation with trichloromethane and precipitation with isopropanol. Subsequently, mRNA concentrations were normalized, and reverse transcription was performed to synthesize cDNA using the PrimeScript™ RT Reagent Kit (TaKaRa, Japan) on a T100™ Thermal Cycler (BIO-RAD, USA). Quantitative real-time PCR (qRT-PCR) was carried out using the CFX Opus 96 Real-Time PCR System (BIO-RAD, USA) with SuperReal PreMix Plus SYBR Green (TIANGEN Biotech Co., Ltd., Beijing, China). The thermal cycling conditions consisted of an initial pre-incubation at 95 °C for 5 min, followed by 55 cycles of denaturation at 95 °C for 10 s, annealing at 60 °C for 20 s, and extension at 72 °C for 30 s. The oligonucleotide sequences and their corresponding annealing temperatures are provided in Table S2. Each sample was analyzed in triplicate, and relative quantification was performed using the $2^{-\Delta\Delta Ct}$ method (Livak method). All data were normalized to appropriate reference genes for standardization.

2.9. Data analysis

All data in this study were analyzed using SPSS 22.0 and visualized with GraphPad Prism 8.0 (GraphPad Software, La Jolla, CA, USA). Measurement data are presented as mean ± standard deviation (SD). Normality was assessed using the Shapiro–Wilk test. For normally distributed data, differences between groups were evaluated by one-way analysis of variance (ANOVA) and two-way ANOVA for multiple comparisons. Non-normally distributed data were analyzed using nonparametric methods. A value of $p < 0.05$ was considered statistically significant.

3. Results

3.1. Compound radiofrequency radiation promotes lipid metabolism throughout the body

Utilizing a well-established electromagnetic reverberation chamber platform, we conducted metabolic studies under multi-frequency compound RF-EMR exposure environment. The irradiation protocol and experimental grouping were shown in Fig. S1A. Throughout the exposure period, weekly measurements of body weight, food intake, and water consumption were recorded for all mice. Compared to the Control group, the RF-EMR group exhibited a significant reduction in weight gain (Fig. 1A), although no statistically significant differences were observed in food or water intake between the two groups (Fig. S3). Serum lipid metabolism analysis revealed a significant decrease in low-density lipoprotein (LDL) and triglyceride (TG) levels, while high-density lipoprotein (HDL) showed an increasing trend that did not reach statistical significance (Fig. 1C). Additionally, malonyl-CoA (MCA) levels were reduced, whereas total cholesterol (TC) remained unchanged (Fig. 1B, C). Evaluation of serum adipokine profiles indicated a significant increase in adiponectin concentration in the RF-EMR group. Although leptin levels exhibited an upward trend, the difference was not statistically significant (Fig. 1B). Collectively, these findings demonstrate that composite radiofrequency radiation exposure effectively attenuates the rate of body weight gain in mice without influencing total nutrient intake.

3.2. Compound radiofrequency radiation activates UCP1 in adipose tissue to promote lipid metabolism

To clarify the effects of compound radiofrequency radiation on adipose tissue structure and function, we examined the morphological characteristics of brown adipose tissue (BAT) and inguinal white adipose tissue (WAT) in mice following exposure. Histopathological analysis revealed that, compared to the Control group, the interscapular BAT in the RF-EMR group displayed a significant decrease in adipocyte diameter and an increase in adipocyte number per field of view (Fig. 1D). Similarly, inguinal WAT also exhibited reduced adipocyte diameter and increased cell density (Fig. S1D, E). Furthermore, both mRNA and protein expression of uncoupling protein 1 (UCP1) were significantly upregulated in BAT and WAT of the RF-EMR group, with a more substantial increase observed in BAT (Fig. 2 C, S1C). Additionally, adiponectin levels in BAT were significantly elevated in the RF-EMR group following radiation exposure, whereas leptin expression remained unchanged. In contrast, both adiponectin and leptin were markedly increased in inguinal WAT (Fig. 2B, S2A). MCA content in BAT of the RF-EMR group was significantly reduced, accompanied by a pronounced decrease in acetyl-CoA carboxylase (ACC) activity. Similarly, MCA levels in inguinal WAT were also significantly lower after irradiation, though ACC activity did not exhibit significant alteration (Fig. 2F, G). These results indicated that compound radiofrequency radiation stimulated adipokine secretion from adipose tissue and enhanced uncoupling protein 1 (UCP1) expression, thereby promoted metabolic activity within adipose tissue.

3.3. The adiponectin signaling pathway is involved in the process of hepatic lipid metabolism promoted by compound radiofrequency radiation

Based on the observed alterations in serum and adipose tissue adipokine profiles, we proposed that adiponectin may play a mediating role

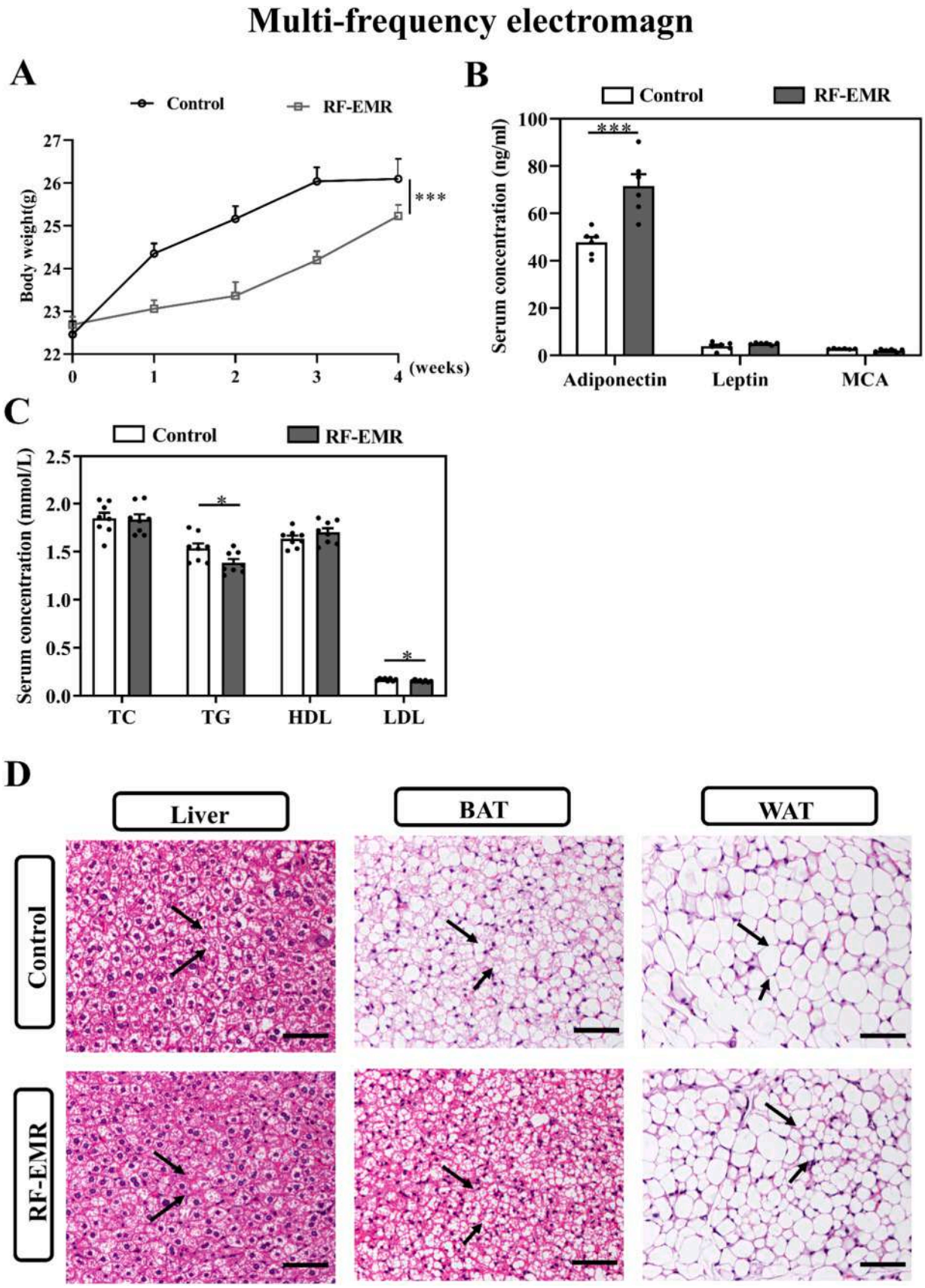


Fig. 1. Mouse model of compound radiofrequency radiation and the level of serum lipid metabolism. A Weight during the experiment (n = 10 each group); B The adiponectin, leptin, MCA levels in serum (n = 6 each group); C Serum levels of HDL, LDL, TG, TC after the compound radiofrequency radiation (n = 8 each group); D Hematoxylin-eosin staining results of liver, BAT and WAT, Scale bar = 50 μm; $^{*}P < 0.05$, $^{***}P < 0.001$.

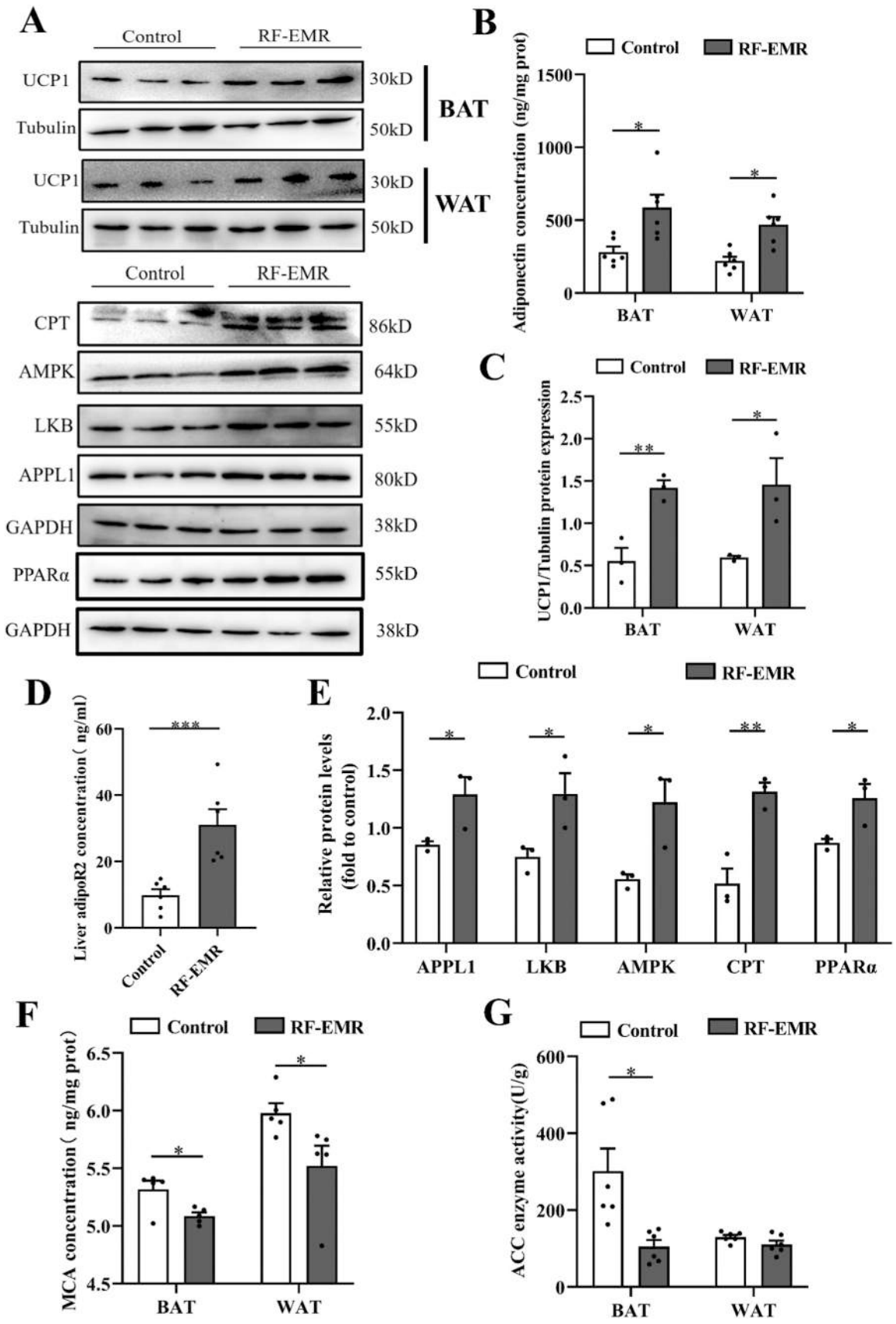


Fig. 2. Compound radiofrequency radiation activated adipose tissue and liver lipid metabolism. A The western blotting bands of BAT, WAT and liver; B The adiponectin and leptin level in BAT and WAT (n = 6 each group); C The protein level of UCP1 in BAT and WAT (n = 3 each group); D The adiponR2 levels in liver (n = 6 each group); E The quantitative analysis of adiponectin pathway protein in liver (n = 3 each group); F The MCA level in BAT and WAT (n = 5 each group); G The ACC enzyme activity levels in liver (n = 6 each group); $^{*}P < 0.05$, $^{**}P < 0.01$, $^{***}P < 0.001$.

in the regulation of lipid metabolism induced by compound radiofrequency radiation in mice. Histological examination of liver morphology revealed no significant structural changes in hepatocytes following radiofrequency radiation exposure. Hepatocyte membranes remained intact, and nuclear structures were clearly delineated without evident abnormalities (Fig. 1D). Subsequently, we examined adiponectin receptors in the liver and observed a significant upregulation following radiation exposure (Fig. 2D). Concurrently, proteins involved in the adiponectin signaling pathway—including APPL1, LKB1, AMPK, PPARα, and CPT—exhibited significantly elevated expression levels (Fig. 2E). Compared to the Control group, the RF-EMR group showed a marked reduction in MCA content and ACC enzyme activity in the liver (Fig. S2B, C). These results collectively suggested that compound radiofrequency radiation enhanced hepatic lipid metabolism through activation of the adiponectin signaling pathway.

3.4. Compound radiofrequency radiation promotes lipid metabolism in obese mice

Building upon previous findings demonstrated that triple-frequency compound radiofrequency radiation reduced the rate of body weight gain and enhanced lipid metabolism in both adipose tissue and liver in normal mice, we further investigated whether such exposure could elicit similar metabolic improvements in obese mice. The irradiation protocol and experimental grouping are summarized in Fig. S1A. Body weight monitoring results revealed that, compared to the HFD group, the RF-HFD group exhibited a significant reduction in weight gain, with a particularly pronounced decrease observed during the first week of irradiation. Notably, age-matched normal mice subjected to the same radiation protocol showed consistent changes in body weight (Fig. 3A). Following irradiation, the RF-HFD group exhibited a significant reduction in both epididymal white adipose tissue (e-WAT) and inguinal white adipose tissue (i-WAT) coefficients compared to the HFD group, whereas the brown adipose tissue (BAT) coefficient was significantly increased. The liver coefficient showed a decreasing trend, although this did not reach statistical significance. Similarly, the Control group demonstrated lower liver, e-WAT, and i-WAT coefficients relative to the HFD group, along with a higher BAT coefficient (Fig. 3E).

Serum lipid metabolism analysis revealed that, compared to the HFD group, the RF-HFD group exhibited a significant increase in high-density lipoprotein (HDL) levels, along with marked reductions in low-density lipoprotein (LDL), total cholesterol (TC), triglycerides (TG), and acetyl-CoA (ACA) following radiation exposure (Fig. 3C, F). In comparison with the Control group, the HFD group showed decreased HDL and elevated levels of LDL, TC, TG, malonyl-CoA (MCA), and ACA (Fig. 3C–F). These alterations are consistent with characteristic blood lipid changes associated with high-fat diet-induced hyperlipidemia mice (Li et al., 2020). Simultaneously, compared to the Control group, the RF-EMR group exhibited a significant increase in high-density lipoprotein (HDL) and reductions in total cholesterol (TC), triglycerides (TG), and acetyl-CoA (ACA) levels (Fig. 3C, F). Furthermore, serum adiponectin levels were elevated in the RF-HFD group relative to the HFD group following radiation exposure (Fig. 3B). These results are consistent with those observed in previous experiments, suggesting that the lipid metabolism-enhancing effects of radiofrequency radiation may not exhibit significant age-related variation.

3.5. Compound radiofrequency radiation increases lipid metabolism in adipose tissue in obese mice

To investigate the effects of compound radiofrequency radiation on various adipose tissues in obese mice, we examined brown adipose tissue (BAT), epididymal white adipose tissue (e-WAT), and inguinal white adipose tissue (i-WAT). Histological analysis via HE staining revealed that, compared to the Control group, adipocytes in BAT, e-WAT, and i-WAT of the RF-EMR group were more densely packed, whereas those in the HFD group displayed a looser arrangement. Additionally, the RF-HFD group exhibited a higher adipocyte density and reduced cell diameter relative to the HFD group (Fig. 4 A, S2F). Analysis of triglyceride levels demonstrated that, compared to the Control group, the RF-EMR group exhibited significantly reduced triglyceride content in BAT and i-WAT, whereas the HFD group showed markedly elevated triglyceride levels in BAT, e-WAT, and i-WAT. Relative to the HFD group, the RF-HFD group displayed a significant decrease in triglyceride accumulation in both BAT and i-WAT (Fig. 4B–D). Evaluation of adipokine expression revealed that adiponectin levels were significantly higher in BAT and i-WAT of the RF-EMR group compared to the Control group. In contrast, the HFD group exhibited a substantial reduction in adiponectin expression in i-WAT. Furthermore, the RF-HFD group showed a significant increase in adiponectin levels in BAT relative to the HFD group (Fig. 5C).

Previous studies have indicated that compound radiofrequency radiation enhanced lipid metabolism in adipocytes. Western blot analysis of UCP1 expression revealed that, compared to the Control group, the RF-EMR group exhibited significantly elevated UCP1 levels in BAT, e-WAT, and i-WAT. the HFD group showed a marked reduction in UCP1 protein content in BAT and i-WAT. Relative to the HFD group, the RF-HFD group demonstrated significantly increased UCP1 expression in both BAT and i-WAT (Fig. 5A, B).

MCA and ACA are important intermediates in both the catabolic and anabolic pathways of triglycerides, and serve as critical biomarkers for assessing lipid metabolism. Additionally, the enzymatic activities of CPT and ACC represent essential indicators for evaluating metabolic flux and regulation. Compared to the Control group, the RF-EMR group displayed significantly elevated CPT enzyme activity in BAT, reduced MCA content and ACC enzyme activity in i-WAT, and increased ACA content and CPT enzyme activity in i-WAT, whereas no significant alterations were detected in e-WAT. Relative to the HFD group, the RF-HFD group exhibited markedly decreased MCA levels and ACC enzyme activity, along with increased CPT enzyme activity in BAT; reduced MCA content and ACC enzyme activity, and elevated ACA content and CPT enzyme activity in i-WAT. In e-WAT, only MCA content and ACC enzyme activity were significantly reduced (Fig. 5D–G). These findings indicated that compound radiofrequency radiation promoted lipid metabolism within adipose tissues and stimulated the release of adipokines, thereby enhanced systemic lipid metabolism.

3.6. Compound radiofrequency radiation promotes liver lipid metabolism via the adiponectin signaling pathway in obese mice

The aforementioned results suggested that compound radiofrequency radiation exerted a comparable regulatory effect on lipid metabolism in obese mice. Histological examination of liver tissue revealed the presence of numerous lipid droplets in both the HFD and RF-HFD groups. However, the RF-HFD group displayed less severe hepatic steatosis, characterized by fewer and smaller lipid droplets relative to the HFD group. Masson's trichrome staining indicated notable fibrosis in both HFD and RF-HFD groups, yet the RF-HFD group exhibited milder fibrotic changes. In contrast, no pathological features of fatty liver disease were observed in the age-matched Control and RF-EMR groups (Fig. 6 A, S2E). Following radiation exposure, the RF-EMR group demonstrated significantly reduced triglyceride levels compared to the Control group, while the RF-HFD group exhibited markedly lower triglyceride levels relative to the HFD group (Fig. 6D). Analysis of adiponectin signaling pathway proteins revealed that, compared to the Control group, the RF-EMR group showed significantly elevated expression levels of adiponectin, adiponectin receptor, APPL1, CPT, LKB1, and AMPK. In comparison to the HFD group, the RF-HFD group displayed significantly increased protein expression of adiponectin, adiponectin receptor, APPL1, and CPT, along with an upward trend in LKB1 and AMPK expression (Fig. 6B, E).

We further quantified hepatic levels of MCA and ACA, as well as the

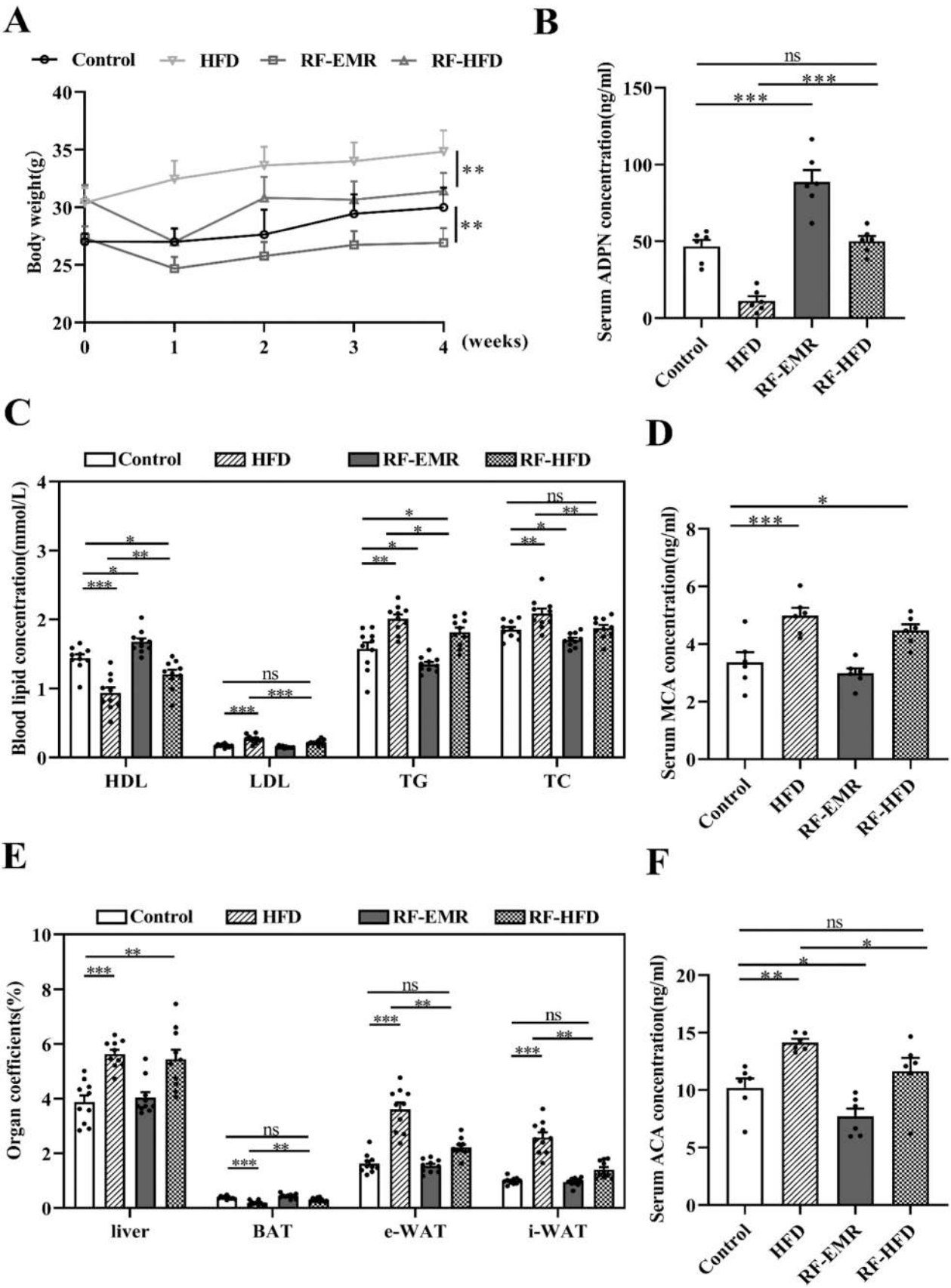


Fig. 3. Establishment of an obese mouse model with radio-frequency radiation and the level of serum lipid metabolism. A Weight during the radiation experiment (n = 10 each group); B Serum levels of adiponectin (n = 6 each group); C Serum levels of HDL, LDL, TG, TC after the radiation experiment (n = 10 each group); D The MCA levels in serum (n = 6 each group); E The organ coefficients (tissue weight/body weight) of mouse liver, BAT, i-WAT and e-WAT after the radiation experiment (n = 10 each group); F Serum levels of ACA (n = 6 each group). $^{*}P < 0.05$, $^{**}P < 0.01$, $^{***}P < 0.001$.

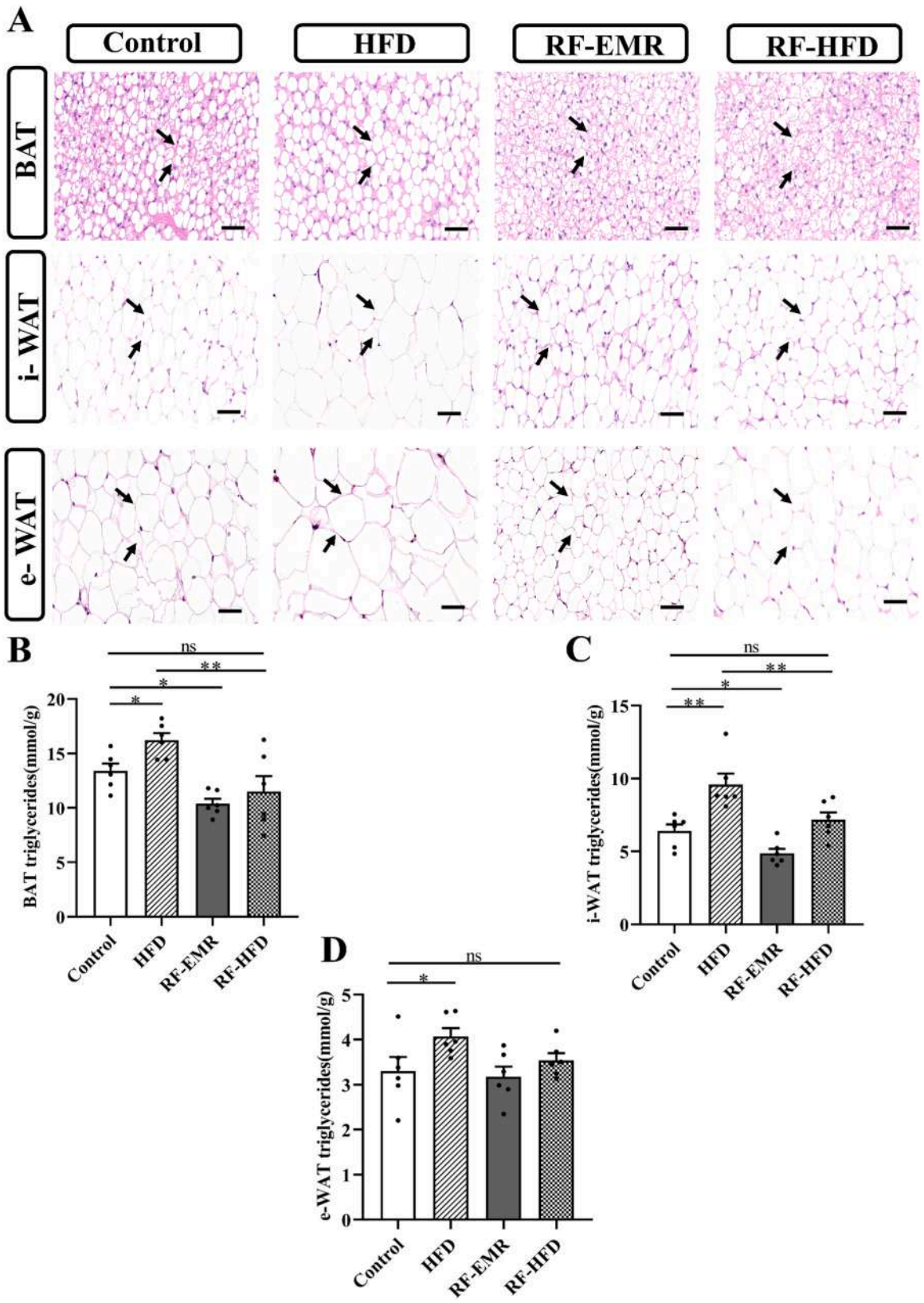


Fig. 4. Compound radiofrequency radiation reduced the amount of triglycerides in adipose tissue. A HE staining results of WAT, i-WAT and e-WAT, Scale bar = 100 μm; B The triglyceride levels in BAT (n = 6 each group); C The triglyceride levels in i-WAT (n = 6 each group); D The triglyceride levels in e-WAT (n = 6 each group). $^{*}P < 0.05$, $^{**}P < 0.01$.

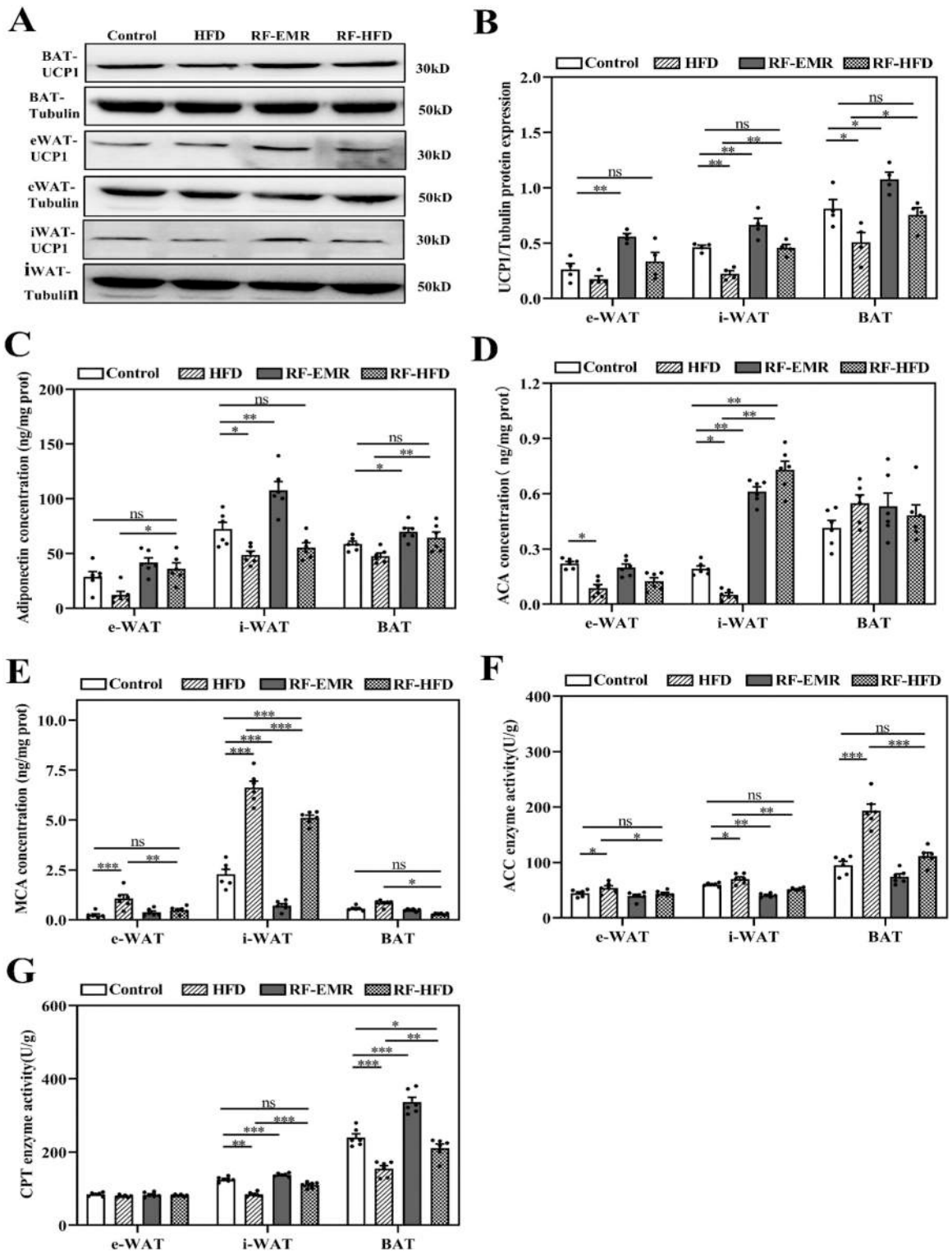


Fig. 5. Compound radiofrequency radiation activated adipose tissue UCP1 and released adipokines in obese mouse. A Western blotting bands of adiponectin pathway protein; B The UCP1 levels in BAT, i-WAT and e-WAT (n = 4 each group); C The adiponectin levels in BAT, i-WAT and e-WAT (n = 6 each group); D The ACA levels in BAT, i-WAT and e-WAT (n = 6 each group); E The MCA levels in BAT, i-WAT and e-WAT (n = 6 each group); F The ACC enzyme activity levels in BAT, i-WAT and e-WAT(n = 6 each group); G The CPT enzyme activity levels in BAT, i-WAT and e-WAT(n = 6 each group). $^{*}P < 0.05$, $^{**}P < 0.01$, $^{***}P < 0.001$.

enzymatic activities of ACC and CPT. The results demonstrated that, compared to the Control group, the RF-EMR group exhibited a significant increase in CPT activity and ACA content, alongside a marked reduction in ACC activity and MCA levels. In the RF-HFD group, ACC activity and MCA content were significantly lower than those in the HFD group, while CPT activity and ACA levels showed an increasing trend that did not reach statistical significance (Fig. 6F, G). These findings indicated that compound radiofrequency radiation also modulated hepatic lipid metabolism in obese mice through the adiponectin signaling pathway.

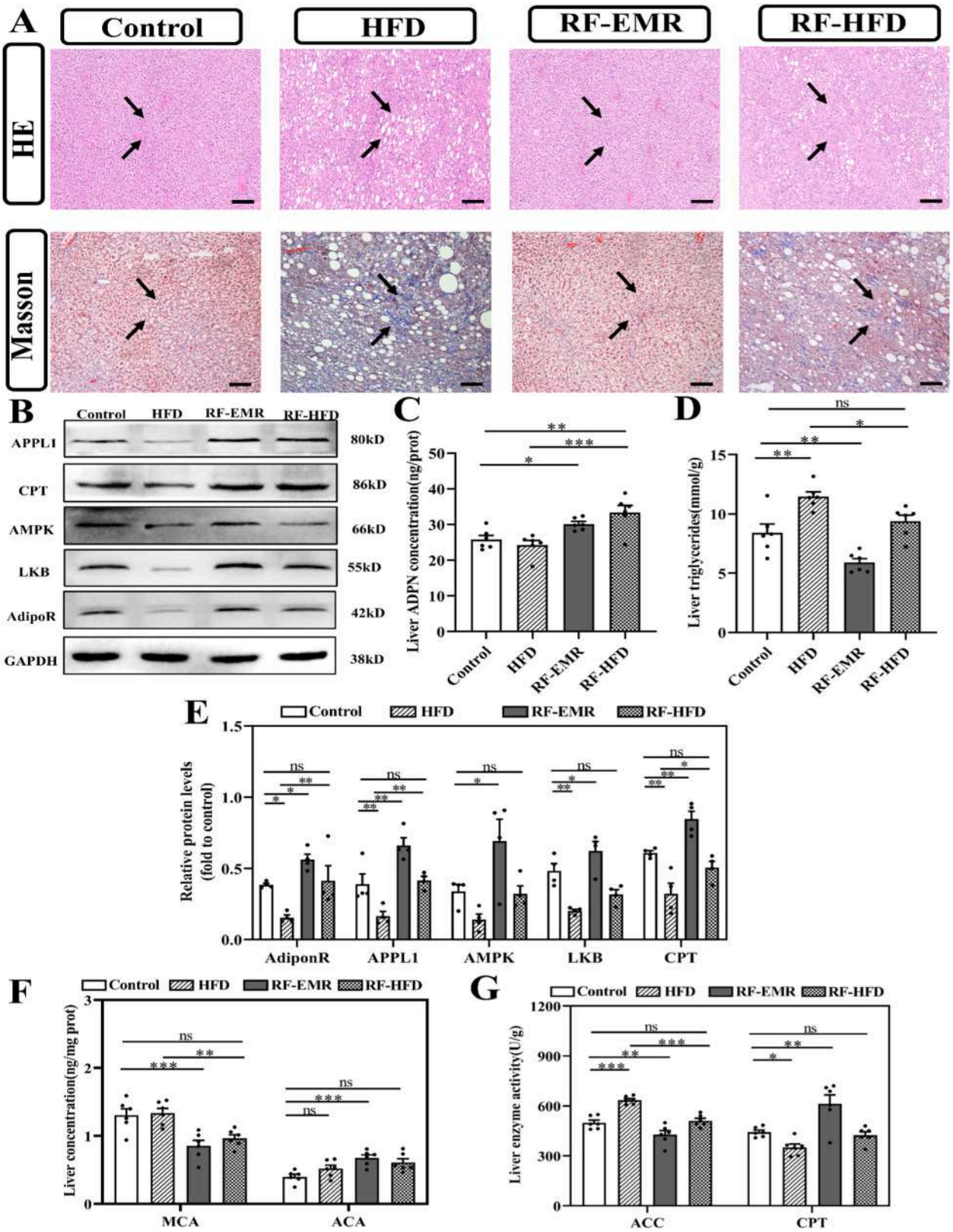


Fig. 6. Compound radiofrequency radiation promoted hepatic lipid metabolism via the adiponectin signaling pathway in obese mouse. A HE staining and Masson's trichrome staining of liver after radiation, HE: Scale bar = 200 μm, Masson: Scale bar = 100 μm; B The Western blotting bands of adiponectin pathway protein in liver; C The adiponectin level in liver (n = 6 each group); D The triglycerides in liver (n = 6 each group); E The quantitative analysis of adiponectin pathway protein in liver (n = 4 each group); F The MCA and ACA levels in liver (n = 6 each group); G The ACC and CPT enzyme activity in liver (n = 6 each group). $^{*}P < 0.05$, $^{**}P < 0.01$, $^{***}P < 0.001$.

4. Discussion

In recent years, the health effects of radiofrequency radiation have garnered significant scholarly attention. A substantial body of literature has demonstrated that radiofrequency radiation disrupted endocrine function, induced central nervous system impairment, and caused damage to other organs and tissues within homeostatic systems, thereby exerted various adverse physiological effects (Xu et al., 2010; Eskandani, Zibaii, 2024; Pardhiya et al., 2022; Hasan et al., 2021). However, most existing studies have focused exclusively on single-frequency radiofrequency radiation exposures, with limited investigation into the impacts and underlying mechanisms of multi-frequency compound radiofrequency radiation. Furthermore, while considerable research has addressed the influence of radiofrequency radiation on emotional and cognitive functions (Zhou et al., 2024; Narayanan et al., 2019; Zhang et al., 2017), relatively few studies have explored its metabolic effects—particularly regarding lipid metabolism. With the widespread adoption of communication devices and continuous advancement of communication technologies (Mortazavi et al., 2014), individuals are increasingly subjected to prolonged exposure to compound radiofrequency radiation environments, which poses potential health implications. Frequencies such as 0.9 GHz, 1.5 GHz, and 2.65 GHz represent key bands extensively utilized in modern telecommunications, resulting in frequent public exposure (Tan et al., 2021; Hao et al., 2023). This study aims to enhance our understanding of the biological effects of multi-frequency electromagnetic environments and to elucidate the mechanisms through which long-term radiofrequency radiation influences lipid metabolism.

In this study, body weight monitoring of mice exposed to compound radiofrequency radiation revealed a significant reduction in weight gain during the first week post-exposure, with continued differences observed in subsequent weeks, diminishing by the fourth week. Analysis of serum lipid metabolism indicators showed decreased levels of triglycerides (TG) and low-density lipoprotein (LDL), alongside increased high-density lipoprotein (HDL), suggesting that compound radiofrequency radiation modulated lipid metabolism. Furthermore, a significant elevation in serum adiponectin levels was observed following radiation, accompanied by an increase in leptin. Previous studies have established that serum adiponectin levels are positively correlated with HDL and inversely correlated with LDL and TG, which is consistent with the present findings (Tsubakio-Yamamoto et al., 2012; Ng et al., 2007). To further verify the impact of compound radiofrequency radiation on lipid metabolism, we subjected it to the same multi-frequency radiation exposure in obese mice. The results demonstrated that the RF-HFD group exhibited a significant reduction in body weight during the first week of irradiation. Following radiation exposure, the RF-HFD group displayed decreased organ indices for e-WAT and i-WAT, along with an increased index for BAT, compared to the HFD group. Serological analysis indicated that, relative to the HFD group, the RF-HFD group showed significantly lower serum levels of TG, TC, LDL, and ACA, while HDL and adiponectin levels were elevated. Similarly, compared to the Control group, the RF-EMR group exhibited decreased TG, TC, and ACA, along with increased HDL and adiponectin. The above results indicated that compound radiofrequency radiation reduced serum lipid metabolic indices and enhanced systemic lipid metabolism levels through adiponectin and other adipokines, ultimately led to attenuated weight gain in mice following radiation exposure.

Most studies on radiofrequency radiation have focused on oxidative stress across various tissues and organs. Meanwhile, adipocytes characterized by abundant lipid droplets and relatively low protein content pose technical challenges for protein extraction. Thus, research concerning adipose tissue and its implications for lipid metabolism remains limited. This study is the first to specifically investigated adipose tissue under compound radiofrequency radiation, demonstrated that compound radiofrequency radiation exposure increased serum levels of adipokines, including adiponectin. Adiponectin, a peptide hormone secreted by adipose tissue, exhibited anti-diabetic, anti-atherosclerotic, and anti-inflammatory properties. It also plays a beneficial role in regulating hepatic glucose and lipid metabolism. In previous studies, we observed an increase in cell number and a decrease in cell diameter within irradiated adipose tissue. Based on these morphological changes, it was hypothesized that compound radiofrequency radiation may enhance lipid metabolism and reduce lipid droplet accumulation in adipocytes. Furthermore, measurements of UCP1 expression revealed significant elevations in both mRNA and protein levels in BAT and WAT. Additionally, we observed a reduction in MCA and the activity of ACC in BAT, as well as decreased MCA in WAT. These findings suggested that compound radiofrequency radiation inhibited the synthesis of fatty acids and triglycerides in adipocytes. Upon irradiation, the levels of adiponectin in BAT increased, along with elevations in both adiponectin and leptin contents in WAT. In subsequent obesity model studies, we observed increased cellular compactness in BAT, e-WAT, and i-WAT in the RF-HFD group post-irradiation, which was consistent with our earlier experimental findings. A similar trend was shown in irradiated mice of the same age (not fed a high-fat diet). Compared to the HFD group, the RF-HFD group exhibited significantly reduced triglycerides in BAT and i-WAT, accompanied by a marked increase in UCP1 protein expression. Additionally, the activities of MCA and ACC were decreased in BAT, e-WAT, and i-WAT. In i-WAT, ACA was elevated, while CPT activity was enhanced in both BAT and i-WAT. Notably, in the RF-HFD group, only the adiponectin in BAT was significantly increased. These results suggested that compound radiofrequency radiation promoted fatty acid catabolism in adipose tissue, reduced triglyceride in adipocytes, and stimulated the release of adiponectin and other adipokines, thereby contributing to the regulation of systemic lipid metabolism. Furthermore, we observed that BAT and i-WAT, which are located closer to the body surface, were more significantly affected by compound radiofrequency radiation compared to e-WAT, which is situated deeper within the body. Whether this differential effect is associated with the selected frequency band, radiation dosage, or potential absorption of radiofrequency energy by the murine surface fur, among other factors, remains to be further investigated.

The findings of this study demonstrated that compound radiofrequency radiation stimulated the release of adiponectin from adipose tissue, thereby modulated systemic lipid metabolism. Previous studies have indicated that adiponectin binds to its receptors (adiponectin receptor 1, adiponectin receptor 2, and T-cadherin) and activated downstream signaling proteins, ultimately influencing the expression and activity of key metabolic enzymes. The liver, as a central organ for both the synthesis and breakdown of triglycerides, represented a major target of adiponectin action. Given the focus of this research on lipid metabolism, the liver was selected as the primary target organ for investigating the effects of adiponectin. We observed that compound radiofrequency radiation did not induce any structural alterations in the liver. Hepatic cells maintained regular arrangement, intact membranes, and clear nuclei following irradiation. Furthermore, the expression of key proteins involved in the adiponectin signaling pathway—including adiponectin receptor, APPL1, LKB1, AMPK, and PPAR-α—was significantly upregulated in the liver after radiation exposure. Concurrently, the protein level of CPT, a critical enzyme in fatty acid β-oxidation, was markedly elevated. In contrast, the intermediate metabolite MCA and the activity of ACC were significantly reduced. In the obesity model study, steatosis and hepatocyte ballooning were observed in both the HFD group and the RF-HFD group. The HFD group exhibited a significant increase in hepatic triglyceride levels. However, the severity of fatty lesions and the concentration of triglycerides in the liver were markedly lower in the irradiated RF-HFD group compared to the HFD group. Liver fibrosis, which is a key indicator of fatty liver disease progression, was also evident in high-fat-fed mice. Notably, the extent of fibrosis was significantly reduced in the RF-HFD group relative to the HFD group, suggested that compound radiofrequency radiation attenuated fatty liver-associated fibrosis. At the same time, we also observed

that the adiponectin signaling pathway was activated in the RF-HFD group, which enhanced the ACA level and CPT enzyme activity related to hepatic triglyceride decomposition, and decreased the MCA level and ACC enzyme activity related to hepatic triglyceride synthesis. These results indicated that compound radiofrequency radiation enhanced triglyceride catabolism and suppressed anabolic processes in the liver through the adiponectin signaling pathway, thereby ameliorated hepatic steatosis in obese mice and promoted systemic lipid metabolism.

In conclusion, our findings suggested that compound radiofrequency radiation induced the secretion of adiponectin and other adipokines from adipose tissue. These adipokines, particularly adiponectin, were subsequently transported to the liver via the circulatory system. Through the adiponectin signaling pathway, this process promoted triglyceride catabolism while simultaneously suppressing triglyceride anabolism in hepatic tissues. This mechanism contributes to systemic lipid metabolism regulation, ultimately manifesting as attenuated weight gain in murine models. The observed metabolic effects potentially extend to obese individuals, indicating a broader applicability of this phenomenon.

However, this study had several limitations. Firstly, we observed that the effects of compound radiofrequency radiation varied across different adipose tissues, which may be related to the specific frequency bands and dosages used. Further experiments are required to confirm this hypothesis. Secondly, although the mice used in the two experiments were of different ages, the results were consistent, suggesting that the effects of compound radiofrequency radiation are not age-dependent. Nevertheless, the lack of experiments involving aged mice represents a limitation of this study, which we plan to address in future research. Thirdly, while we demonstrated that compound radiofrequency radiation modulates hepatic lipid metabolism via the adiponectin signaling pathway, we didn't establish a definitive causal relationship between the radiation and adiponectin pathway. Future studies will employ more advanced techniques, such as gene knockout models, to validate this mechanism. Fourthly, the radiation dose applied in this study corresponds to the highest permissible environmental safety threshold as defined by the International Commission on Non-Ionizing Radiation Protection (ICNIRP). This level exceeds both the daily public and occupational exposure limits and was selected strictly as an experimental safety reference. In subsequent investigations, we intend to conduct systematic studies involving lower doses to further expand and diversify the current body of research. Finally, this study didn't investigate female mice or perform interventions targeting the adiponectin pathway. We intend to conduct additional experiments to address these gaps and expand potential applications.

5. Conclusions

In summary, our study demonstrated that long-term compound radiofrequency radiation upregulated the expression of UCP1 in adipose tissue, enhanced lipid metabolism within adipocytes, and stimulated the secretion of adiponectin and other adipokines. Subsequently, these adipokines activated the adiponectin signaling pathway in the liver, led to improved hepatic lipid metabolism. Ultimately, this systemic modulation ameliorated overall lipid homeostasis and attenuated the rate of weight gain. These effects were also observed in obese mice, wherein long-term compound radiofrequency radiation significantly alleviated the severity of hepatic steatosis and reduced liver fibrosis. These findings provided novel insights into the potential application of non-invasive strategies for the management of obesity.

Abbreviations

ACA	Acetyl -CoA
ACC	Acetyl-CoA carboxylase
AMPK	Adenosine 5'-monophosphate (AMP)-activated protein kinase
APPL1	Adaptor Protein, Phosphotyrosine Interacting With PH Domain And Leucine Zipper 1
BAT	Brown adipose tissue
CPT	Carnitine palmityl transferase
e-WAT	Epididymal white adipose tissue
HDL	High-density lipoprotein
HFD	High-fat feeding
i-WAT	Inguinal white adipose tissue
LDL	Low-density lipoprotein
LKB	Liver kinase B1
MCA	Malonyl-CoA
PPARα	Perixisome proliferator-activated receptor alpha
RF-EMR	Radiofrequency electromagnetic radiation
TC	Total cholesterol
TG	Triglyceride
UCP1	Uncoupling protein 1

Declarations

Ethic approval and consent to participate All the animal experiments in the study were approved by Animal Laboratory of Laboratory animal center Academy of Military Medical Sciences (IACUC-DWZX-2024–518).

CRediT authorship contribution statement

Menghua Li: Formal analysis, Data curation. **Lihui Zhang:** Data curation. **Xuelong Zhao:** Data curation. **Guofu Dong:** Writing – review & editing, Project administration, Funding acquisition. **Jing Xu:** Writing – original draft, Methodology, Formal analysis, Data curation, Conceptualization. **Xinyu Wang:** Formal analysis, Data curation. **Changzhen Wang:** Writing – review & editing, Project administration, Funding acquisition.

Consent for publication

Not applicable.

Funding

This study received no special funding from any funding agency in the public, private or non-profit sectors.

Declaration of Competing Interest

The authors declare that they have no known competing financial interests or personal relationships that could have appeared to influence the work reported in this paper.

Appendix A. Supporting information

Supplementary data associated with this article can be found in the online version at doi:10.1016/j.ecoenv.2025.119016.

Data availability

Data will be made available on request.

References

Ahmad, B., Vohra, M.S., Saleemi, M.A., Serpell, C.J., Fong, I.L., Wong, E.H., 2021. Brown/Beige adipose tissues and the emerging role of their secretory factors in improving metabolic health: the batokines. Biochimie 184, 26–39.
Caballero, B., 2019. Humans against obesity: who will win? Adv. Nutr. 10 (_1), S4–S9.
Chand, S., Tripathi, A.S., Dewani, A.P., Sheikh, N.W.A., 2024. Molecular targets for management of diabetes: remodelling of White adipose to brown adipose tissue. Life Sci. 345, 122607.

Chen, X., Zhang, Y., Li, L., Li, S., Zhang, J., 2022. Treadmill running alleviates adipose tissue browning and lipolysis in rats with heart failure. J. Physiol. Biochem. 78 (2), 323–334.
Choi, H.M., Doss, H.M., Kim, K.S., 2020. Multifaceted physiological roles of adiponectin in inflammation and diseases. Int. J. Mol. Sci. 21 (4), 1219.
Dyck, D.J., Heigenhauser, G.J., Bruce, C.R., 2006. The role of adipokines as regulators of skeletal muscle fatty acid metabolism and insulin sensitivity. Acta Physiol. 186 (1), 5–16.
Eskandani, R., Zibaii, M.I., 2024. Unveiling the biological effects of radio-frequency and extremely-low frequency electromagnetic fields on the central nervous system performance. Bioimpacts 14 (4), 30064.
Fragopoulou, A.F., Polyzos, A., Papadopoulou, M.D., Sansone, A., Manta, A.K., Balafas, E., Kostomitsopoulos, N., Skouroliakou, A., Chatgilialoglu, C., Georgakilas, A., Stravopodis, D.J., Ferreri, C., Thanos, D., Margaritis, L.H., 2018. Hippocampal lipidome and transcriptome profile alterations triggered by acute exposure of mice to GSM 1800 MHz mobile phone radiation: an exploratory study. Brain Behav. 8 (6), e01001.
Furtado-Filho, O.V., Borba, J.B., Dallegrave, A., Pizzolato, T.M., Henriques, J.A., Moreira, J.C., Saffi, J., 2014. Effect of 950 MHz UHF electromagnetic radiation on biomarkers of oxidative damage, metabolism of UFA and antioxidants in the livers of young rats of different ages. Int. J. Radiat. Biol. 90 (2), 159–168.
Ghadge, A.A., Khaire, A.A., Kuvalekar, A.A., 2018. Adiponectin: a potential therapeutic target for metabolic syndrome. Cytokine Growth Factor Rev. 39, 151–158.
Hao, Y., Liu, W., Liu, Y., Liu, Y., Xu, Z., Ye, Y., Zhou, H., Deng, H., Zuo, H., Yang, H., Li, Y., 2023. Effects of nonthermal radiofrequency stimulation on neuronal activity and neural circuit in mice. Adv. Sci. 10 (11), e2205988.
Hardell, L., Koppel, T., 2022. Electromagnetic hypersensitivity close to mobile phone base stations - a case study in Stockholm, Sweden. Rev. Environ. Health 38 (2), 219–228.
Hasan, I., Amin, T., Alam, M.R., Islam, M.R., 2021. Hematobiochemical and histopathological alterations of kidney and testis due to exposure of 4G cell phone radiation in mice. Saudi J. Biol. Sci. 28 (5), 2933–2942.
Kadowaki, T., Yamauchi, T., Kubota, N., Hara, K., Ueki, K., Tobe, K., 2006. Adiponectin and adiponectin receptors in insulin resistance, diabetes, and the metabolic syndrome. J. Clin. Invest 116 (7), 1784–1792.
Karpale, M., Kummu, O., Kärkkäinen, O., Lehtonen, M., Näpänkangas, J., Herfurth, U.M., Braeuning, A., Rysä, J., Hakkola, J., 2023. Pregnane x receptor activation remodels glucose metabolism to promote NAFLD development in obese mice. Mol. Metab. 76, 101779.
Koppel, T., Ahonen, M., Carlberg, M., Hardell, L., 2022. Very high radiofrequency radiation at skeppsbron in Stockholm, Sweden from mobile phone base station antennas positioned close to pedestrians' heads. Environ. Res. 208, 112627.
Küçer, N., Pamukçu, T., 2014. Self-reported symptoms associated with exposure to electromagnetic fields: a questionnaire study. Electro Biol. Med. 33 (1), 15–17.
Levitt, B.B., Lai, H., 2010. Biological effects from exposure to electromagnetic radiation emitted by cell tower base stations and other antenna arrays. Environ. Rev. 18, 369–395.
Li, J., Wu, H., Liu, Y., Yang, L., 2020. High fat diet induced obesity model using four strains of mice: kunming, C57BL/6, BALB/c and ICR. Exp. Anim. 69 (3), 326–335.
Liu, X., Zhang, Z., Song, Y., Xie, H., Dong, M., 2023. An update on brown adipose tissue and obesity intervention: function, regulation and therapeutic implications. Front. Endocrinol. 13, 1065263.
Magkos, F., Mittendorfer, B., 2009. Stable isotope-labeled tracers for the investigation of fatty acid and triglyceride metabolism in humans in vivo. Clin. Lipido 4 (2), 215–230.
Men, J., Zhang, L., Peng, R., Li, Y., Li, M., Wang, H., Zhao, L., Zhang, J., Wang, H., Xu, X., Dong, J., Wang, J., Yao, B., Guo, J., 2023. Metformin ameliorates 2.856 GHz microwave- radiation-induced reproductive impairments in Male rats via inhibition of oxidative stress and apoptosis. Int. J. Mol. Sci. 24 (15), 12250.
Miyagishima, K., Hiramitsu, S., Kato, S., Kato, Y., Kitagawa, F., Teradaira, R., Shinohara, R., Mori, K., Kimura, H., Ueda, T., Ohtsuki, M., Morimoto, S., Hishida, H., 2007. Efficacy of atorvastatin therapy in ischaemic heart disease - effects on oxidized low-density lipoprotein and adiponectin. J. Int. Med. Res. 35 (4), 534–539.
Mortazavi, S.A., Tavakkoli-Golpayegani, A., Haghani, M., Mortazavi, S.M., 2014. Looking at the other side of the coin: the search for possible biopositive cognitive effects of the exposure to 900 MHz GSM mobile phone radiofrequency radiation. J. Environ. Health Sci. Eng. 12, 75.
Narayanan, S.N., Jetti, R., Kesari, K.K., Kumar, R.S., Nayak, S.B., Bhat, P.G., 2019. Radiofrequency electromagnetic radiation-induced behavioral changes and their possible basis. Environ. Sci. Pollut. Res. Int. 26 (30), 30693–30710.
Ng, T.W., Watts, G.F., Barrett, P.H., Rye, K.A., Chan, D.C., 2007. Effect of weight loss on LDL and HDL kinetics in the metabolic syndrome: associations with changes in plasma retinol-binding protein-4 and adiponectin levels. Diabetes Care 30 (11), 2945–2950.
Pardhiya, S., Gaharwar, U.S., Gautam, R., Priyadarshini, E., Nirala, J.P., Rajamani, P., 2022. Cumulative effects of manganese nanoparticle and radiofrequency radiation in Male wistar rats. Drug Chem. Toxicol. 45 (3), 1395–1407.
Tan, S., Wang, H., Xu, X., Zhao, L., Zhang, J., Dong, J., Yao, B., Wang, H., Hao, Y., Zhou, H., Gao, Y., Peng, R., 2021. Acute effects of 2.856 GHz and 1.5 GHz microwaves on spatial memory abilities and CREB-related pathways. Sci. Rep. 11 (1), 12348.
Tsubakio-Yamamoto, K., Sugimoto, T., Nishida, M., Okano, R., Monden, Y., Kitazume-Taneike, R., Yamashita, T., Nakaoka, H., Kawase, R., Yuasa-Kawase, M., Inagaki, M., Nakatani, K., Masuda, D., Ohama, T., Matsuyama, A., Nakagawa-Toyama, Y., Ishigami, M., Komuro, I., Yamashita, S., 2012. Serum adiponectin level is correlated with the size of HDL and LDL particles determined by high performance liquid chromatography. Metabolism 61 (12), 1763–1770.
Vaidya, H., Goyal, R.K., Cheema, S.K., 2013. Anti-diabetic activity of swertiamarin is due to an active metabolite, gentianine, that upregulates PPAR-γ gene expression in 3T3-L1 cells. Phytother. Res. 27 (4), 624–627.
Volkow, N.D., Tomasi, D., Wang, G.J., Vaska, P., Fowler, J.S., Telang, F., Alexoff, D., Logan, J., Wong, C., 2011. Effects of cell phone radiofrequency signal exposure on brain glucose metabolism. JAMA 305 (8), 808–813.
Xiao, F., Jiang, H., Li, Z., Jiang, X., Chen, S., Niu, Y., Yin, H., Shu, Y., Peng, B., Lu, W., Li, X., Li, Z., Lan, S., Xu, X., Guo, F., 2023. Reduced hepatic bradykinin degradation accounts for cold-induced BAT thermogenesis and WAT browning in Male mice. Nat. Commun. 14 (1), 2523.
Xu, S., Zhou, Z., Zhang, L., Yu, Z., Zhang, W., Wang, Y., Wang, X., Li, M., Chen, Y., Chen, C., He, M., Zhang, G., Zhong, M., 2010. Exposure to 1800 MHz radiofrequency radiation induces oxidative damage to mitochondrial DNA in primary cultured neurons. Brain Res. 1311, 189–196.
Xue, L., Sun, J., Sun, Y., Wang, Y., Zhang, K., Fan, M., Qian, H., Li, Y., Wang, L., 2024. Maternal brown rice diet during pregnancy promotes adipose tissue browning in offspring via reprogramming PKA signaling and DNA methylation. Mol. Nutr. Food Res. 68 (8), e2300861.
Yu, G., Tang, Z., Chen, H., Chen, Z., Wang, L., Cao, H., Wang, G., Xing, J., Shen, H., Cheng, Q., Li, D., Wang, G., Xiang, Y., Guan, Y., Zhu, Y., Liu, Z., Bai, Z., 2020. Long-term exposure to 4G smartphone radiofrequency electromagnetic radiation diminished Male reproductive potential by directly disrupting Spock3-MMP2-BTB axis in the testes of adult rats. Sci. Total Environ. 698, 133860.
Zhang, J.P., Zhang, K.Y., Guo, L., Chen, Q.L., Gao, P., Wang, T., Li, J., Guo, G.Z., Ding, G. R., 2017. Effects of 1.8 GHz radiofrequency fields on the emotional behavior and spatial memory of adolescent mice. Int. J. Environ. Res. Public Health 14 (11), 1344.
Zhou, G.Q., Wang, X., Gao, P., Qin, T.Z., Guo, L., Zhang, Z.W., Huang, Z.F., Lin, J.J., Jing, Y.T., Wang, H.N., Wang, C.P., Ding, G.R., 2024. Intestinal microbiota via NLRP3 inflammasome dependent neuronal pyroptosis mediates anxiety-like behaviour in mice exposed to 3.5 GHz radiofrequency radiation. Sci. Total Environ. 927, 172391.